Remodeling in bone without osteocytes: Billfish challenge bone structure–function paradigms

Ayelet Atkins[a,1], Mason N. Dean[b,1], Maria Laura Habegger[c], Phillip J. Motta[c], Lior Ofer[a], Felix Repp[b], Anna Shipov[a], Steve Weiner[d], John D. Currey[e], and Ron Shahar[a,2]

[a]Koret School of Veterinary Medicine, The Robert H. Smith Faculty of Agriculture, Food and Environment, The Hebrew University of Jerusalem, Rehovot 76100, Israel; [b]Department of Biomaterials, Max Planck Institute of Colloids and Interfaces, 14476 Potsdam, Germany; [c]Department of Integrative Biology, University of South Florida, Tampa, FL 33613; [d]Department of Structural Biology, Weizmann Institute of Science, Rehovot 76100, Israel; and [e]Department of Biology, University of York, York YO10 5DD, United Kingdom

Edited by David B. Burr, Indiana University School of Medicine, Indianapolis, IN, and accepted by the Editorial Board September 19, 2014 (received for review July 3, 2014)

A remarkable property of tetrapod bone is its ability to detect and remodel areas where damage has accumulated through prolonged use. This process, believed vital to the long-term health of bone, is considered to be initiated and orchestrated by osteocytes, cells within the bone matrix. It is therefore surprising that most extant fishes (neoteleosts) lack osteocytes, suggesting their bones are not constantly repaired, although many species exhibit long lives and high activity levels, factors that should induce considerable fatigue damage with time. Here, we show evidence for active and intense remodeling occurring in the anosteocytic, elongated rostral bones of billfishes (e.g., swordfish, marlins). Despite lacking osteocytes, this tissue exhibits a striking resemblance to the mature bone of large mammals, bearing structural features (overlapping secondary osteons) indicating intensive tissue repair, particularly in areas where high loads are expected. Billfish osteons are an order of magnitude smaller in diameter than mammalian osteons, however, implying that the nature of damage in this bone may be different. Whereas billfish bone material is as stiff as mammalian bone (unlike the bone of other fishes), it is able to withstand much greater strains (relative deformations) before failing. Our data show that fish bone can exhibit far more complex structure and physiology than previously known, and is apparently capable of localized repair even without the osteocytes believed essential for this process. These findings challenge the unique and primary role of osteocytes in bone remodeling, a basic tenet of bone biology, raising the possibility of an alternative mechanism driving this process.

anosteocytic bone | osteon | bone toughness | damage-driven remodeling | fish skeleton

Bone forms the stiff, load-bearing framework of the body of vertebrates. The current paradigm of bone biology is that the microdamage that accumulates in bone—the result of repeated loading over long periods of time—is prevented from reaching failure levels by "remodeling," a physiologic maintenance process by which packets of damaged bone material are removed, then replaced by new, undamaged tissue (1). The most crucial role in the remodeling sequence is thought to be played by the osteocytes, the cells residing within the bone matrix, which sense local increases in strain (or strain energy density) caused by microcrack accumulation, then initiate and coordinate remodeling once a defined threshold is reached (2, 3). First, surface-residing osteoclasts (bone-resorbing cells) are recruited to invade and erode packets of damaged tissue within the bone material, a process that creates visible resorption cavities. Osteoblasts (bone-building cells) are then recruited to these eroded areas, and fill them concentrically from the periphery inwards with new bone, leaving only a small central canal for the passage of blood vessels and nerves (4). This "repair by replacement" process alters bone's ultrastructural morphology, leaving behind lamellate, nearly circular "secondary osteons" (Fig. 1 *A–D*). Because subsequent secondary osteons do not respect each other's borders, heavily remodeled tissue, which forms particularly in situations of large load magnitudes and/or cyclic loading, bears a characteristic morphology of overlapping osteons (Fig. 1 *C* and *D*), a structural record of vigorous remodeling (ref. 2; *SI Text*).

Considering the pivotal role of osteocytes in remodeling and that remodeling is believed to be essential for the proper long-term function of bone, it is surprising that the bones of almost all members of the huge group of extant neoteleost fish—close to 50% of all vertebrates—are completely devoid of osteocytes (anosteocytic) (Fig. 1*E*) (5, 6). According to the current tenets of bone biology, because local internal strains are believed to be sensed by osteocytes alone (3, 7), remodeling in anosteocytic fish species would either not occur at all, be driven by something other than damage, or be stochastic in nature (i.e., "undirected"). The former option, lack of remodeling, is supported by the fact that the bone of most fish species examined to date has been shown to be featureless (i.e., to lack traces of remodeling; e.g., Fig. 1*E*), particularly in comparison with mammalian bone (e.g., Fig. 1 *A–D*) (5, 6, 8–11). From a functional point of view, however, there are many reasons to expect that both osteocytic and anosteocytic fishes should need to remodel their bones: Remodeling occurs in a wide assortment of aquatic and terrestrial amniote species (4, 12, 13); fish experience large loads on their skeletons (e.g., bite forces can exceed 300 N, and fish

Significance

A fundamental paradigm of bone biology is that the remodeling process—by which bones detect and repair damage—is orchestrated by osteocytes. The bones of most extant fish, however, lack these cells and should be unable to repair damage in their bones. We provide evidence for intense remodeling in the anosteocytic bone of billfishes, such as swordfish and marlin. Our observations challenge the central axiom that osteocytes alone are responsible for remodeling, suggesting alternate mechanisms in bone physiology and/or variation in the roles of bone cells. In addition, billfish bone exhibits an array of striking material properties that distinguish it from mammalian bone despite having similar composition, underlining that skeletal biology concepts are limiting when based on mammalian tissues alone.

Author contributions: A.A., M.N.D., M.L.H., P.J.M., S.W., J.D.C., and R.S. designed research; M.L.H. acquired animals; A.A., M.L.H., L.O., A.S., J.D.C., and R.S. performed research; F.R. contributed new reagents/analytic tools; A.A., M.N.D., and R.S. analyzed data; and M.N.D. and R.S. wrote the paper.

The authors declare no conflict of interest.

This article is a PNAS Direct Submission. D.B.B. is a guest editor invited by the Editorial Board.

[1]A.A. and M.N.D. contributed equally to this work.

[2]To whom correspondence should be addressed. Email: ron.shahar1@mail.huji.ac.il.

This article contains supporting information online at www.pnas.org/lookup/suppl/doi:10.1073/pnas.1412372111/-/DCSupplemental.

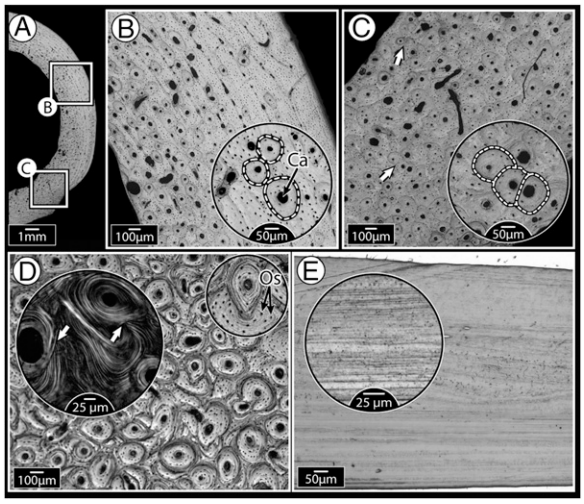

Fig. 1. Mammalian bone ultrastructure, showing morphological evidence for remodeling, compared with relatively "featureless" fish bone. (*A*) Cross-section of dog femoral midshaft with localized areas showing primary and remodeled bone (secondary osteons). (*B*) Higher magnification of the upper boxed region in *A*, showing isolated, nonoverlapping osteons (borders indicated by dashed lines) present in otherwise lamellar (layered) primary bone tissue. Every osteon is organized around a central Haversian canal (Ca); smaller black dots are osteocyte lacunae. (*C*) Higher magnification of the lower boxed region in *A*, showing much higher osteonal density, with many overlapping osteons (secondary osteons, shown by arrows, and in more detail in the inset image), indications of tissue remodeling. (*D*) Horse third metatarsal bone showing heavy remodeling, evidenced by extensive osteonal overlap. *Inset* polarized microscopy image illustrates how osteonal lamellae are "interrupted" by lamellae of new osteons (white arrows). The smaller *Inset* image highlights the high concentration of osteocyte lacunae (Os), visible as small black dots throughout the tissue. (*E*) Tilapia opercular bone which, like most fish bone examined to date, has a simple layered ultrastructure, even at higher magnification (*Inset*). This species is anosteocytic (i.e., lacks osteocytes entirely); in contrast, the mammalian tissues in *A*–*D* all have numerous osteocytes.

mass-specific bite forces are the highest recorded among vertebrates; ref. 14); and in vivo physiologic strains measured in fish bone are within the same range as those of mammals, and with considerably higher strain rates (15).

Although fish (both osteocytic and anosteocytic) have been shown to respond to changing loading conditions by altering bone external morphology (the process of "modeling," performed only on external and internal surfaces; see *SI Text*), there has been to date no definitive morphological evidence of remodeling within the bone material (*SI Text*). We examined the anosteocytic skeletons of billfishes, species with bone that we argue is at the extreme end of the need for remodeling (Fig. 2 and Fig. S1). The billfishes (Xiphiidae and Istiophoridae) have long life spans (up to several decades), and can reach large body sizes and high swimming speeds (up to 600 kg and 75 km/h, respectively, in some species) (16, 17). The large pointed rostra or "bills" from which the fishes get their common name—formed from sword- or spear-shaped, elongated upper jaw bones—are used to strike and stun a variety of prey (16, 18, 19). These factors suggest that the long rostra regularly sustain repeated high forces, which result in high stresses and strains and, therefore, have a substantial demand for superior bone material properties (e.g., unique resistance to failure) and/or remodeling to ensure long-term bone health and function. We focus our analysis on several billfish species, including some with bills reaching impressive lengths (~0.5 m or a quarter of the body length of the fish in blue marlin, *Makaira nigricans*, and more than 1.0 m or half of body length in swordfish, *Xiphias gladius*) (Fig. 2 and Fig. S1). Billfish rostra therefore represent an extreme example of anosteocytic bone, loaded heavily and cyclically in cantilever bending over the animals' long lifespans, and likely in need of regular remodeling to avoid failure. The five species examined provide a broad palette of body sizes and bill lengths in a closely related group of fishes (Fig. 2 and Fig. S1) and, therefore, are an ideal system to investigate correlations among body/bill size, reported activity level, and evidence for remodeling.

Structural Properties of the Bone of the Billfish Rostrum

The internal architecture of the rostral bone of all billfish species examined here bears striking resemblance to mammalian secondary osteonal bone, in stark contrast to the bone of fish previously examined, and bone from billfish opercula (Figs. 1–3 and *SI Text*). Bone cross-sections are densely populated by "osteon-like" structures that are lamellate and nearly circular, possess a central canal, and are surrounded by a slightly crenulated border (a "cement line"). However, whereas mammalian secondary osteons are heavily populated with osteocytes and believed to depend on them for their formation (7, 20, 21), billfish "osteons" are entirely devoid of these cells, thus presenting a striking variation on the classical appearance of mammalian secondary osteons (compare osteons in Figs. 1 and 3). The cement lines of "anosteocytic osteons" (a term we will use to distinguish them from tetrapod osteons) are much brighter than the bone matrix they surround when viewed in back-scattered scanning electron (BSE) microscopy (Fig. 3*B* and insets in Fig. 2 and Fig. S1), suggesting they are comprised of a material with higher mean mineral density (22). Cement lines are a prominent feature of tetrapod secondary osteons and are also reported to be more highly mineralized (and therefore more brittle) than the matrix they surround (23); they are therefore thought to be a major contributor to bone toughness by causing propagating cracks to deflect around rather than cut through osteons (24, 25). Billfish

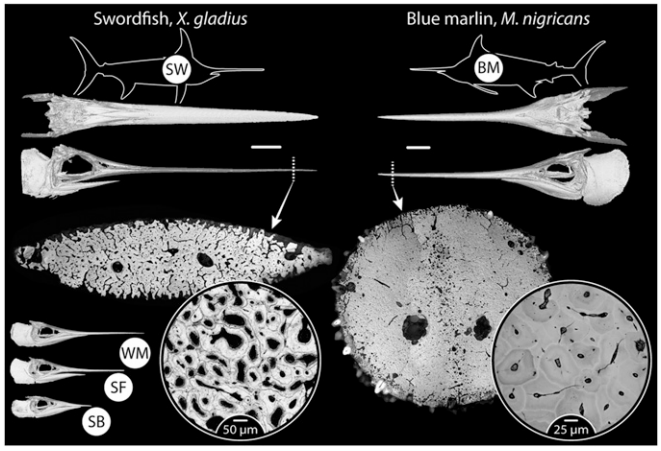

Fig. 2. Gross morphology and ultrastructure of billfish bone. Swordfish (SW) and blue marlin (BM) are shown here; tissue ultrastructure of the additional species examined (SB, shortbill spearfish; SF, sailfish; WM, white marlin) is shown in Fig. S1. The body plan of the fish is shown as a silhouette, with CT scan images beneath showing the skull in dorsal and lateral perspectives (white bars between CT scans = 10 cm). Light microscopy images of distal, whole bill transverse cross-sections are shown beneath CT scans, demonstrating an array of complex ultrastructures, with circular inset images providing a higher magnification of the acellular osteonal tissue (BM, backscatter electron image; SW, light microscopy image). CT scans of crania of the remaining three species in the lower left corner illustrate the variation in relative bill length among species. Two-letter acronyms for each species (in white circles in species' silhouettes) are used also in subsequent figures.

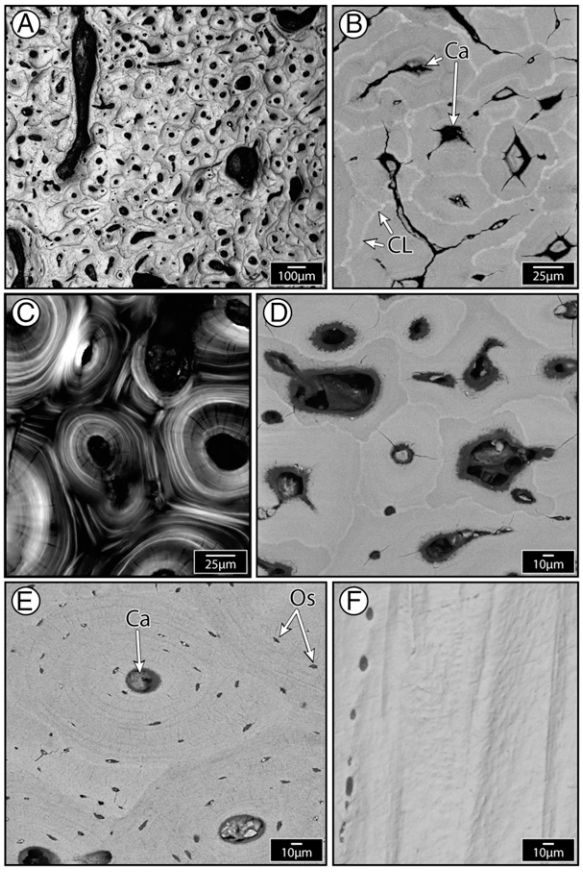

Fig. 3. Evidence for secondary (remodeled) tissue in billfishes. (*A*) Dense osteonal tissue in white marlin (light microscopy). (*B*) Blue marlin osteons (backscatter electron image, BEI): Each osteon has a central canal and is surrounded by a brighter cement line, indicating higher mineral density. (*C*) Swordfish osteons (polarized light), showing concentric lamellar ultrastructure of osteons and the interruption of lamellae by overlapping (i.e., newer) osteons (similar to Fig. 1*D* larger inset). (*D*) Swordfish osteons (BEI). (*E*) Horse osteons (BEI), with the central Haversian canal (Ca) and osteocyte lacunae (Os) indicated. (*F*) Swordfish opercular bone (light microscopy), lacking osteons (similar to Fig. 1*E*). *D*–*F* are the same magnification to facilitate comparison: Billfish rostral bone is characterized by osteons that are significantly smaller than mammalian osteons (compare *D* and *E*) and exhibits far more complex ultrastructure than the simple, layered billfish opercular bone tissue (compare *D* and *F*).

cement lines, compared with those of tetrapods, exhibit much greater grayscale contrast relative to the matrix, suggesting they are either hypermineralized or perhaps relatively collagen-poor or both (23).

Similar to mammalian bone, when billfish osteons are studied under polarized light—the natural birefringence of collagen enabling the visualization of collagen fibril orientation—they exhibit several concentric lamellae around each osteon's central cavity (compare Fig. 3*C* with Fig. 1*D, Inset*). Successive lamellae are alternately bright and dark in appearance, suggesting different underlying collagen orientations (as in "Type II" mammalian osteons): Collagen layers oriented in line with the osteonal long-axis appear dark and those with collagen layers oriented off-axis (>45° relative to the long axis) appear bright (26) (Fig. 1*C*). These images illustrate that, where osteons overlap, the continuity of the lamellae of the "background" (older) osteon is interrupted by the presence of the "foreground" (newer) osteon. This morphology provides convincing evidence that this is secondary osteonal tissue, and not simply bone exceptionally dense with nonoverlapping primary osteons (structures developing in primary bone, not via remodeling; see *SI Text*).

Despite gross shape similarity between osteocytic and anosteocytic osteons, from a histomorphometric perspective, billfish osteons are strikingly different from those of mammals (27, 28), having a spatial density that is effectively an order of magnitude higher (ranging between 150 and 250 osteons/mm^2) and being ~50–90% smaller (typically less than 110 μm wide, with areas 0.004–0.021 mm^2) (Figs. 2, 3 *A*–*D*, and 4*A*). Both billfish and mammalian osteonal networks are comprised of long osteonal central canals (Haversian canals in mammals), oriented mostly in line with the long axis of the bone, and shorter transverse canals (Volkmann's canals in mammals), linking adjacent central canals (Fig. 4 *A* and *B*) (29, 30). However, the central canals of billfish osteons are comparatively small, ranging from 17 to 50 μm in diameter, less than 50% the diameter of the analogous mammalian Haversian canals (Fig. 4*A*). The high density of osteons (and therefore the high density of central canals) results in compact bone tissue with high porosity, ranging between 8 and

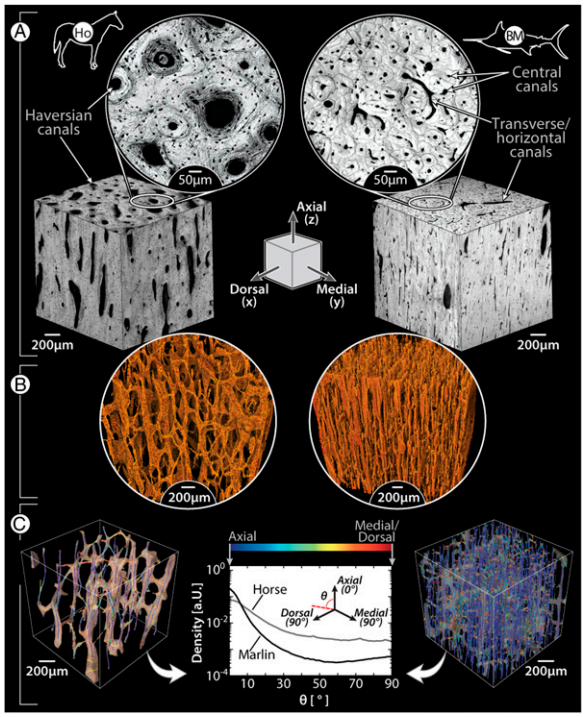

Fig. 4. Comparison of vascular canal morphology in mammals and billfishes, using horse limb bone (*Left*) and blue marlin rostral bone (*Right*) as examples; the illustrated schematic in the center of *A* shows the anatomical orientation of all images, with the axial/longitudinal axis of the bones running from the top to bottom of the page. (*A*) Light microscopy images of the orthogonal faces of bone cubes (*Inset* images show higher magnification of the transverse plane, perpendicular to the axial direction); note the size difference between horse and blue marlin osteons and the presence of osteocytes in the horse image (small black dots surrounding each canal). (*B*) Volume-rendering of a microCT scan of each species' canal network; note the comparatively large horizontal canals in blue marlin. (*C*) Volume-rendered skeletonization of canal networks, with canal segments color-coded according to orientation relative to the axial direction (blue, axial; red, perpendicular to axial, i.e., medial/dorsal). The frequency plot of these orientations illustrates that the majority of canals are oriented axially (0°) in both species; however, blue marlin also show a tendency toward a second peak at 90°, whereas horse exhibit more canal segments with intermediate angles (0° > θ > 90°). Horizontal canals in blue marlin (e.g., visible in *A*) are obscured by the extremely dense network of vertical canals in the volume renderings in *B* and *C*.

15% even in the most "compact" areas (i.e., in the distal quarter of the bill), and up to even 35% in white marlin. This porosity is at least twice that of mammalian compact bone, even considering the contribution of the lacunar-canalicular system (28, 30). The differences in canal size and density between billfish and mammalian bone result in canal networks with fundamentally different topographies, as illustrated by volume renderings of the canal systems from microcomputed tomography scans of small cubes of billfish bone and of equine cortical bone (Fig. 4 *B* and *C*). Our analysis of canal segment directionality (Fig. 4*C*, *Methods*, and *SI Methods*) shows that the canals in blue marlin bone exhibit a somewhat bimodal distribution, with a strong bias toward the axial direction and a smaller secondary peak at 90° (i.e., horizontal canals), whereas the canals in horse bone, although also mostly axially directed, have a higher frequency of obliquely oriented canals. Although billfish bone obviously lacks the lacunar-canalicular system of tetrapod bone (which links osteocytes within an osteon with each other and the central canal), the high density of billfish bone canals represents a similarly interconnected bone canal network.

The anosteocytic osteons we show here impart a hugely intricate ultrastructure to the bone tissue, far exceeding that observed in any previous microscopy image of fish bone (see *SI Text* for detailed discussion of species previously examined). As in mammals, morphological evidence of remodeling in these species suggests correlations with ontogeny and activity. For example, the distal bill has a higher density of secondary osteons (i.e., is more remodeled) than the base (e.g., in the blue marlin, 181 ± 78 SD osteons/mm^2 at a location three-quarters of the bill's length from the base, compared with 76 ± 36 SD osteons/mm^2 at a location one-quarter of the bill's length from the base). This observation leads us to suggest that the tip is the oldest portion of the bill and/or where most microdamage accumulates. Furthermore, secondary osteons are less prevalent or absent in bones that are apparently under less rigorous mechanical demands, such as the skeletons of smaller, less active species (e.g., carp, tilapia; Fig. 1*E*), the opercula of all billfish species examined here (e.g., Fig. 3*D*), and the shorter rostrum of the shortbill spearfish (Fig. 2 and Fig. S1). Moss (6) and Ørvig (31) reported no secondary tissue in the many bony fish species they examined, with the latter going as far as to state that secondary osteons were "as a rule absent in fishes" (p. 331); our data show this assertion to be incorrect. Nevertheless, it is possible that remodeling is not ubiquitous in fishes: The examples of remodeled bone presented here occur within a small group of fishes with exceptional cranial morphologies, body sizes, and performance, and all previous suggestions of remodeling were found only within anosteocytic acanthopterygian fishes (*SI Text*). Multiple actinopterygian orders contain active and/or large fish species (e.g., exceeding 1.5 m in length), providing ideal fodder for future examinations to untangle relationships among remodeling, mechanical demands and phylogeny.

If we assume that the broad structural characteristics and dynamics of the remodeling process are similar among vertebrate taxa, with osteoclasts digging resorption cavities in existing bone and osteoblasts filling them concentrically from the outside in, the morphologies we observe suggest remodeling in billfishes and mammals may differ in some fundamental aspects. In mammals, resorption cavity size dictates the size of the resulting osteon (27). The comparatively small osteons of billfishes may reflect the known morphological and functional differences between osteoclasts of advanced teleosts and those of mammals: In contrast to the giant multinucleate osteoclasts of mammals that excavate deep pits during resorption, fish osteoclasts are primarily mononucleate, extremely flat, and considerably smaller, performing instead a smooth (nonexcavating) resorption (32, 33). In addition, the larger osteons in mammals could also be related to the presence of osteocytes, which may participate in determining the size of osteons.

Osteon dimensions could also be related to the size of the damaged regions they are replacing. In mammals, osteon diameters are often larger than observed microcrack lengths (27, 34, 35), supporting the idea that the sizes of secondary osteons are a function of the amount of local microdamaged tissue they replace. Osteon size in fishes could suggest a difference in the average sizes of zones in need of repair and, therefore, an inherently different response to fatigue failure; however, the physiological and material responses of fish bone to microdamage (e.g., whether microcracks form at all in vivo) are at present unknown and require further investigation.

Mechanical Properties of the Bone of the Billfish Rostrum

The composition (e.g., organic and inorganic content) and structure of bone dictate its ability to manage load. Our understanding of the parameter space of bone function is shaped almost entirely by data from terrestrial mammal bone material, with limited perspective as to whether and how bone properties change according to ecology and functional role (but see refs. 36–38). The mechanical properties of fish bone have been only rarely examined, with most works investigating osteocytic fish bone and all only reporting stiffness (e.g., not properties relating to yield behavior or toughness). The available data point to fish bone being much more compliant than tetrapod bone, with elastic moduli in the range of 5–8 GPa (8, 39, 40), less than half of mammalian bone stiffness (5–25 GPa) (4), although fish bone consists of the same basic building blocks as tetrapod bone (mineralized collagen fibrils and water) (11, 41).

We performed mechanical tests on small, same-sized beams of bone from the five billfish species, and (for comparison) from additional species for which material property data already exist: an anosteocytic teleost (tilapia, *Oreochromis aureus*), an osteocytic teleost (carp, *Cyprinus carpio*), horse (*Equus caballus*), and human (*Homo sapiens*); our data for these latter four species agreed with

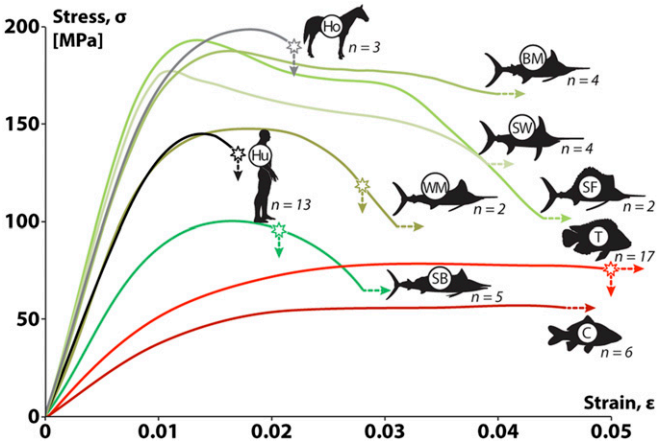

Fig. 5. Average stress–strain curves for similar-sized bone beams tested in bending, for two mammal species (Ho, horse; Hu, human), five billfish species (see Fig. 2 for acronyms), and two additional bony fishes (C: carp, osteocytic bone; T: tilapia, anosteocytic bone). Young's modulus is the slope of the initial, linear portion of the stress–strain curve. Stars on curves indicate the average fracture stress/strain for those samples that fractured during testing. Lines that lack stars or continue past the fracture point (i.e., fish species) continued to strain without failure until the displacement limit of the testing machine. Note that, although billfish bone (excepting shortbill, SB) tended to be as stiff as mammal bone (i.e., to have a similar initial slope), it reached considerably larger postyield strains, similar to other fish species (C, carp; T, tilapia). Numbers next to each species indicate number of beams tested.

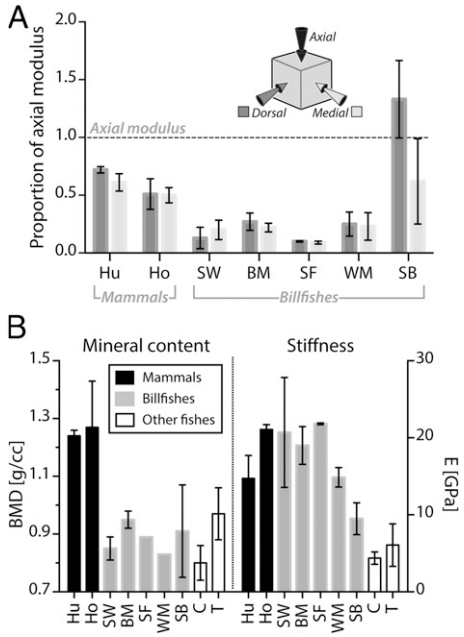

Fig. 6. Mineral content, stiffness, and anisotropy of bone tissue from mammalian and fish species (see Figs. 2 and 5 for species acronyms). (*A*) Bone stiffness anisotropy. For each species, the medial and dorsal moduli are plotted relative to the axial modulus (dashed horizontal line at 1.0); values above or below this line indicate orthogonal moduli that are higher or lower than the axial modulus, respectively. Billfish bone, like mammalian bone, is considerably stiffer in the axial direction (i.e., in line with the bill's long axis), with shortbill again being an exception. (*B*) Mineral content (BMD) is higher in mammalian species than fish species; however, the stiffness (E) of billfish bone is similar to that of mammalian bone and higher than that of other fish species, with shortbill (SB), exhibiting an intermediate stiffness (see also Fig. 5). Note the different tissue morphology of shortbill relative to other billfish bone in Fig. S1 and see Fig. 4 for tissue ultrastructure associated with the different anatomical orientations. Horse data are from ref. 48 and human data from ref. 49.

previous work (4, 8, 42). Results show that the bone of billfish possesses mechanical properties that can be considered a unique blend of fish and mammalian bone characteristics (Figs. 5–6). The stiffness and yield strain of billfish bone are similar to those of mammals, ranging from 12 to 20 GPa and 0.7 to 0.8%, respectively (Fig. 5). However, although mammalian bone typically fails at strains of ∼2%, billfish bone material typically failed at strains greater than 3–4%, in other words, deforming twice as much before fracture. In fact, most billfish samples remained unfractured even at the maximum displacements possible for our mechanical testing machine (∼5% strain) (Fig. 5).

Mammalian osteonal bone exhibits a strong orientation dependence of its stiffness (mechanical anisotropy), being 1.3–2.0 times stiffer along the longitudinal axes of osteons (i.e., longitudinal axis of long bones) compared with the orthogonal orientations (Fig. 6*A*). Our results for billfish bone, based on compression testing of cubes in three orthogonal directions, revealed similar anisotropy, biased toward the axial direction however to a more extreme degree, being on average 6.3 times (and up to 11 times) stiffer when loaded in line with the longitudinal axis of the bill (Fig. 6*A*). This effect seems linked to the presence and arrangement of the acellular osteons, because shortbill spearfish bone (with less pronounced osteonal structure and orientation) was most stiff in the medial direction (Fig. 6*A*), and mechanical anisotropy was not seen in species that lack osteons (e.g., tilapia and carp) (8).

Variations in material properties across tetrapod mineralized tissues reflect, to a large degree, variations in their compositions. Mineral content, in particular, plays an important role in dictating material properties, having a positive relationship with material stiffness and stress at yield, but a negative relationship with the work to fracture and ultimate strain of mineralized vertebrate tissues (36–38). The mineral density of billfish bone, reasonably consistent among the different billfish species tested here (0.9–1.0 g/cc), was also similar to the average levels reported for other fish species, both osteocytic and anosteocytic (0.75–1.00 g/cc) (8, 39) (Fig. 6*B*). This level of mineralization is impressively low given the extreme and nonlinear dependence of stiffness on mineral content in vertebrate mineralized tissues and in comparison with the mineral density of the human samples measured here (1.24 g/cc; Fig. 6*B*) and of most mature mammalian bone (∼1.20–1.30) (4). The similarity among the mineral densities determined for billfish and other fish species and the high stiffness and extreme anisotropy of billfish bone, compared with the stiffness and mechanical isotropy reported for other fish bones, leads us to conclude that billfish bone stiffness is the consequence of structural features (e.g., its osteonal structure) rather than higher mineral density.

The large failure strains for billfish bone indicate impressively high material toughness, allowing it to deform considerably before fracturing. It has been shown that mineralized biological materials achieve high toughness through their hierarchical structure and composite nature, with tissue ultrastructure creating circuitous, energy-dissipating paths for microcracks to follow, allowing them to deform safely under load, whereas pure mineral would exhibit brittle fracture. It is possible that, similar to tetrapod bone, the hypermineralized cement lines of billfish osteons create a stiffness mismatch with the osteonal tissue they enclose, serving to deflect propagating cracks, however, with the smaller osteons of billfishes creating more complex environments for cracks to navigate. Additionally, the apparently high rate of remodeling in anosteocytic bone could eliminate microdamage more efficiently than in mammalian bone, increasing material toughness by returning the tissue to an undamaged state. A high remodeling rate would also suggest that at any time, more of the bone is "new" and therefore less mineralized (supported by our mineral density data), resulting perhaps in longer postyield regions, as in comparatively poorly mineralized tissues like young mammalian bone and antler. The long postyield region of fish bone allows the tissue a longer period of use following regular fatigue damage, providing more time for the repair process; examination of the response of billfish bone to cyclical loading and the nature of propagation of its microdamage is needed to clarify whether this tissue reacts to regular use in a manner inherently different to tetrapod bone.

Conclusion

The occurrence of remodeling in anosteocytic bone begs reevaluation of one of the most fundamental paradigms of bone biology. If billfish bone is remodeled in response to regular fatigue damage (as is strongly supported by our data), how is the need determined without strain-sensing osteocytes? Remodeling in billfish bone suggests either that fishes possess a different strain sensor than mammals or that the role is not solely managed by osteocytes in vertebrates. Given the particularly high density of central canals of osteons in billfish bone and the apparent lack of need of rich vascular perfusion (i.e., given that there are no osteocytes to nourish; refs. 4, 43, and 44), we suggest that central canal tissues may house the triggers for the repair mechanism, perhaps involving bone lining cells covering the walls of the robust canal system (32), as had been previously proposed for mammalian bone (45). Alternatively, it may be that bone remodeling in billfish is not directed by damage, rather it is either driven by some other process (e.g., tissue age) or is completely stochastic, as has been proposed for a certain proportion of mammalian remodeling (46). However, the association among relative bill length, intensity of remodeling, and bone

material properties seen in billfishes (e.g., the shortbill showing the least stiff, tough and remodeled bone) argues for a remodeling process driven by strain intensity. Investigations of structural changes and cellular recruitment strategies in response to load and damage in both osteocytic and anosteocytic fish bone will provide vital clues to the processes at work, while also broadening our perspectives on fundamental roles of cells in the biology of skeletal tissues.

Methods

A detailed description of methods is provided in *SI Methods*.

Animals and Samples. We examined bills of five billfish species: blue marlin (*M. nigricans*), white marlin (*Kajikia albida*), sailfish *(Istiophorus albicans*), shortbill spearfish (*Tetrapturus angustirostris*), and swordfish (*X. gladius*). Tested samples included transverse sections, cubes, and beams.

Microscopy. Transverse sections of bills were ground, polished, then examined by reflected-light microscopy (25%, 50%, 75%, 95% along the bill), polarized light microscopy (75% location), and scanning electron microscopy (75% location).

Medical and Micro CT Scanning and Quantification of Canal Networks. Heads from all five species were medical CT scanned and volume-rendered in Mimics (Materialise HQ). Cubes of blue marlin bill and horse (*Equus caballus*) third metacarpal bone were micro-CT scanned and canal networks volume-rendered for anatomical investigation in Drishti (sf.anu.edu.au/Vizlab/drishti). Angular data were visualized by color-coding skeletonized canals in 3D by using MayaVi (47) and then summarized in a frequency histogram of canal segment angles (Fig. 4*C*).

Mechanical Testing. Cortical bone beams from the five billfish species (75% location), horse (third metatarsal bone), human (*H. sapiens*, femora and metatarsi), carp (*C. carpio*, opercula), and tilapia (*O. aureus*, opercula) were tested by three-point bending. Load-deformation data were converted to stress and strain by using beam theory, then all beams were micro-CT scanned to determine bone mineral density. Cubes ($2 \times 2 \times 2$ mm) from the densest compact bone in the 75% location of the bills of all billfishes were also tested in compression in all three orthogonal anatomical orientations (Fig. 4).

ACKNOWLEDGMENTS. We thank Paul Zaslansky for performing two high-resolution microCT scans and John Dunlop for insight in crafting the manuscript. Samples were obtained because of the generous assistance of Anna Avrigian, Jim Franks, Eric Prince, Ann Barse, Geoff Walker and David Itano. A.A., L.O., and A.S. were supported by Israel Science Foundation Grant 29/12. M.N.D. was supported by Human Frontier Science Program Young Investigator Grant RGY0067 and Gottfried Wilhelm Leibniz-Preis 2010 DFG - FR 2190/4-1. M.L.H. was supported by the University of South Florida, Guy Harvey Ocean Foundation, and Porter Family Foundation.

1. Frost HM (1969) Tetracycline-based histological analysis of bone remodeling. *Calcif Tissue Res* 3(3):211–237.
2. Frost HM (1987) Bone "mass" and the "mechanostat": A proposal. *Anat Rec* 219(1): 1–9.
3. Schaffler MB, Kennedy OD (2012) Osteocyte signaling in bone. *Curr Osteoporos Rep* 10(2):118–125.
4. Currey JD (2002) *Bones: Structure and Mechanics* (Princeton Univ Press, Princeton, NJ), pp 436.
5. Kölliker A (1859) On the different types in the microscopic structure of the skeleton of osseous fishes. *Proc Biol Sci* 9:656–688.
6. Moss ML (1961) Studies of the acelluar bone of teleost fish. I. Morphological and systematic variations. *Acta Anat (Basel)* 46:343–362.
7. Bonewald LF (2011) The amazing osteocyte. *J Bone Miner Res* 26(2):229–238.
8. Cohen L, et al. (2012) Comparison of structural, architectural and mechanical aspects of cellular and acellular bone in two teleost fish. *J Exp Biol* 215(11):1983–1993.
9. Shahar R, Dean MN (2013) The enigmas of bone without osteocytes. *Bonekey Rep* 2: 343.
10. Enlow DH, Brown SO (1956) A comparative histological study of fossil and recent bone tissues. Part I. *Tex J Sci* 8:405–443.
11. Parenti LR (1986) The phylogenetic significance of bone types in euteleost fishes. *Zool J Linn Soc* 87(1):37–51.
12. Bentolila V, et al. (1998) Intracortical remodeling in adult rat long bones after fatigue loading. *Bone* 23(3):275–281.
13. Castanet J, de Ricqlès A (1986) Sur la relativité de la notion d'ostéones primaires et secondaires et de tissus osseux primaire et secondaire en général [On the relativity of the concept of primary and secondary osteons, and of primary and secondary bone tissues in general]. *Annales de sciences naturelles (Biologie animale, zoologie)* 8:103–109.
14. Grubich JR, Huskey S, Crofts S, Orti G, Porto J (2012) Mega-Bites: Extreme jaw forces of living and extinct piranhas (Serrasalmidae). *Scientific Reports* 2:1009.
15. Lauder GV, Lanyon LE (1980) Functional anatomy of feeding in the bluegill sunfish, *Lepomis macrochirus: In vivo* measurement of bone strain. *J Exp Biol* 84(1):33–55.
16. Nakamura I (1985) Billfishes of the world. *Synopsis No. 125*, (Food Ag Org UN, Rome), Vol 5.
17. Waldford LA (1937) *Marine Game Fishes of the Pacific Coast, Alaska to the Equator* (Univ of California Press, Berkeley).
18. Domenici P, et al. (2014) How sailfish use their bills to capture schooling prey. *Proc Biol Sci* 281(1784):20140444.
19. Wisner R (1958) Is the spear of istiophorid fishes used in feeding? *Pac Sci* 12:60–70.
20. Jacobs CR, Temiyasathit S, Castillo AB (2010) Osteocyte mechanobiology and pericellular mechanics. *Annu Rev Biomed Eng* 12(1):369–400.
21. Xiong J, O'Brien CA (2012) Osteocyte RANKL: New insights into the control of bone remodeling. *J Bone Miner Res* 27(3):499–505.
22. Reid SA, Boyde A (1987) Changes in the mineral density distribution in human bone with age: Image analysis using backscattered electrons in the SEM. *J Bone Miner Res* 2(1):13–22.
23. Skedros JG, Holmes JL, Vajda EG, Bloebaum RD (2005) Cement lines of secondary osteons in human bone are not mineral-deficient: New data in a historical perspective. *Anat Rec A Discov Mol Cell Evol Biol* 286(1):781–803.
24. Ritchie RO, Buehler MJ, Hansma P (2009) Plasticity and toughness in bone. *Phys Today* 62(6):41–47.
25. Launey ME, Chen PY, McKittrick J, Ritchie RO (2010) Mechanistic aspects of the fracture toughness of elk antler bone. *Acta Biomater* 6(4):1505–1514.
26. Bromage TG, et al. (2003) Circularly polarized light standards for investigations of collagen fiber orientation in bone. *Anat Rec B New Anat* 274(1):157–168.
27. Qiu S, Fyhrie DP, Palnitkar S, Rao DS (2003) Histomorphometric assessment of Haversian canal and osteocyte lacunae in different-sized osteons in human rib. *Anat Rec A Discov Mol Cell Evol Biol* 272(2):520–525.
28. Skedros JG, Sorenson SM, Jenson NH (2007) Are distributions of secondary osteon variants useful for interpreting load history in mammalian bones? *Cells Tissues Organs* 185(4):285–307.
29. Cooper DML, Matyas JR, Katzenberg MA, Hallgrimsson B (2004) Comparison of microcomputed tomographic and microradiographic measurements of cortical bone porosity. *Calcif Tissue Int* 74(5):437–447.
30. Currey JD, Shahar R (2013) Cavities in the compact bone in tetrapods and fish and their effect on mechanical properties. *J Struct Biol* 183(2):107–122.
31. Ørvig T (1951) Histologic studies of placoderms and fossil elasmobranchs. *Ark Zool* 2(2):321–454.
32. Witten PE, Huysseune A (2009) A comparative view on mechanisms and functions of skeletal remodelling in teleost fish, with special emphasis on osteoclasts and their function. *Biol Rev Camb Philos Soc* 84(2):315–346.
33. Witten PE, Villwock W (1997) Growth requires bone resorption at particular skeletal elements in a teleost fish with acellular bone (*Oreochromis niloticus*, Teleostei: Cichlidae). *J Appl Ichthyol* 13(4):149–158.
34. Mohsin S, O'Brien FJ, Lee TC (2006) Microcracks in compact bone: A three-dimensional view. *J Anat* 209(1):119–124.
35. Muir P, Johnson KA, Ruaux-Mason CP (1999) In vivo matrix microdamage in a naturally occurring canine fatigue fracture. *Bone* 25(5):571–576.
36. Currey JD (1969) The mechanical consequences of variation in the mineral content of bone. *J Biomech* 2(1):1–11.
37. Currey JD (1988) The effect of porosity and mineral content on the Young's modulus of elasticity of compact bone. *J Biomech* 21(2):131–139.
38. Currey JD (1999) The design of mineralised hard tissues for their mechanical functions. *J Exp Biol* 202(Pt 23):3285–3294.
39. Dean MN, Shahar R (2012) The structure-mechanics relationship and the response to load of the acellular bone of neoteleost fish: A review. *J Appl Ichthyol* 28(3):320–329.
40. Horton JM, Summers AP (2009) The material properties of acellular bone in a teleost fish. *J Exp Biol* 212(Pt 9):1413–1420.
41. Moss ML (1963) The biology of acellular teleost bone. *Ann N Y Acad Sci* 109:337–350.
42. Reilly DT, Burstein AH (1975) The elastic and ultimate properties of compact bone tissue. *J Biomech* 8(6):393–405.
43. Enlow DH (1962) Functions of the Haversian system. *Am J Anat* 110:269–305.
44. Marotti G, Zallone AZ (1980) Changes in the vascular network during the formation of Haversian systems. *Acta Anat (Basel)* 106(1):84–100.
45. Mullender MG, Huiskes R (1997) Osteocytes and bone lining cells: Which are the best candidates for mechano-sensors in cancellous bone? *Bone* 20(6):527–532.
46. Burr DB (2002) Targeted and nontargeted remodeling. *Bone* 30(1):2–4.
47. Ramachandran P, Varoquaux G (2011) Mayavi- 3D visualization of scientific data. *Comput Sci Eng* 13(2):40–51.
48. Shahar R, et al. (2007) Anisotropic Poisson's ratio and compression modulus of cortical bone determined by speckle interferometry. *J Biomech* 40(2):252–264.
49. Espinoza Orías AA, Deuerling JM, Landrigan MD, Renaud JE, Roeder RK (2009) Anatomic variation in the elastic anisotropy of cortical bone tissue in the human femur. *J Mech Behav Biomed Mater* 2(3):255–263.